

Novel metallic and insulating states at a bent quantum Hall junction

M. Grayson,^{1,2} L. Steinke,¹ D. Schuh,^{1,*} M. Bichler,¹ L. Hoeppel,²
J. Smet,² K. v. Klitzing,² D. K. Maude,³ and G. Abstreiter¹

¹Walter Schottky Institut, Technische Universität München, 85748 Garching, Germany

²Max-Planck-Institut für Festkörperforschung, 70569 Stuttgart, Germany

³Grenoble High Magnetic Field Laboratories CNRS, 38042 Grenoble, France

(Dated: February 8, 2020)

A non-planar geometry for studying quantum Hall physics is studied, whereby two quantum Hall (QH) systems are joined at a sharp right angle. At the junction of the two incompressible QH states, a one-dimensional conducting state is expected. Experimentally this junction conductance is observed to vary with the filling factor ν that characterizes the incompressible facets. One state at $\nu = 1/3$ is observed to be metallic – the conductance increases as the temperature T drops. Another state at $\nu = 1, 2$ is strongly insulating as a function of temperature, and yet another state at $\nu = 3, 4$ shows only weak temperature dependence. Upon applying a dc voltage bias along the junction, the differential conductance again shows three qualitatively different behaviors. Differences from planar QH structures are highlighted.

PACS numbers: 71.70.Di, 71.70.Ej, 72.25.Dc

Experimental studies of one-dimensional (1D) conductors are relevant for both nanoelectronics and basic physics. Conductance in semiconductor nanowires [1, 2, 3, 4] is limited by disorder and interactions which can backscatter propagating charge. In chiral 1D systems like quantum Hall (QH) edges [5, 6] charge propagates in only one direction but can be tailored to backscatter and interact at one [7] or several [8] point-like constrictions. More about 1D systems could be learned if two QH edges could be coupled to an extended disorder potential to reconstitute a wire, but soft confinement structures with lithographically defined edges [9] suffer from edge reconstruction [10, 11] and sharp confinement structures include a tunnel barrier [12] which spatially separates forward and reverse movers, reducing both interactions and backscattering.

Here we study a conducting state at the corner of two QH systems joined at a 90° angle, where the corner geometry itself serves as a sharp QH boundary and hosts strongly coupled 1D forward and reverse movers with no barrier in between. At different filling factor ν , both metallic and insulating conductance along the junction are observed as a function of temperature and voltage. The small conductances and length dependence suggest disorder mediated scattering. Most striking is the metallic behavior at $\nu = 1/3$ whereby conductance along the junction increases with decreasing temperature, suggestive of a QH "antiwire" [13, 14]. Such non-planar confinement structures are unconventional for the QH effect, and Hartree calculations of the anticipated 1D dispersion illustrate possible origins of the observed phases.

The bent quantum well is fabricated by epitaxially overgrowing a GaAs/AlGaAs heterostructure on a cleaved corner [15] [Fig. 1(a,b)]. A GaAs well layer is topped with an $\text{Al}_{0.7}\text{Ga}_{0.3}\text{As}$ barrier with modulation doping at a distance $d = 120$ nm, forming an L-shaped

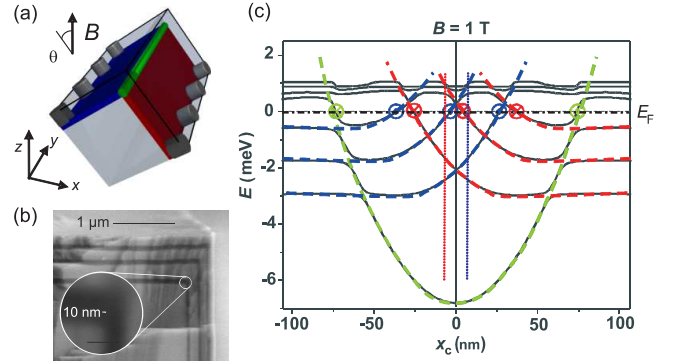


FIG. 1: (a) Schematic of the bent quantum well subjected to a quantizing magnetic field B . The constituent electron systems – QH effect in the facets (blue and red) and 1D corner accumulation (green) – are colored according to their dispersions in panel (c) with contacts in grey. (b) Scanning electron micrograph of a diagnostic corner-overgrowth with alternating AlAs (dark) and GaAs (light) bands. The corner curvature R is sharper than the 10 nm resolution of the electron microscope. (c) Hartree calculations of the dispersion at a sharp corner (black) from Eq. 1, overlaid with left- (blue) and right-facing (red) sharp QH edge dispersions and an accumulation wire dispersion (green). Vertical dotted lines represent the positions of the effective hard walls seen at the corner by electrons in each facet.

heterointerface where electrons are confined. The facets have near-equal densities $n_1 = 1.10 \times 10^{11} \text{ cm}^{-2}$ and $n_2 = 1.28 \times 10^{11} \text{ cm}^{-2}$, and a junction length $L = 2$ mm for sample A ($n_1 = 1.11 \times 10^{11} \text{ cm}^{-2}$, $n_2 = 1.45 \times 10^{11} \text{ cm}^{-2}$, and $L = 4.5$ mm for sample B)[16] with a mobility estimated at around $\mu \sim 5 \times 10^5 \text{ cm}^2/\text{Vs}$. Additional samples showed the same behavior.

A tilted magnetic field B at angle θ can induce the QH effect in both facets. At a conventional QH edge,

the perpendicular field component B induces a gapped incompressible 2D state within each facet, leaving chiral 1D edge channels to carry current at the periphery[5, 6] (Fig. 2, inset). The most prominent gapped states occur when the filling factor $\nu = \hbar n / e B_{\perp}$ is an integer or odd-denominator fraction, and for the integer QH effect, ν also counts the number of 1D edge channels. This Letter considers only equal ν on both facets (for other B orientations and ν ratios, see Ref. [15].)

To understand what sort of 1D states may exist in the bent quantum well, we calculate the dispersion at finite B using the Hartree potential at the corner $V_H(x, z)$ solved at $B = 0$:

$$\left\{ \frac{(\mathbf{p} + e\mathbf{A})^2}{2m^*} + V_H(x, z) \right\} \psi = E\psi \quad (1)$$

Fig. 1(a) shows the Cartesian coordinate orientation, and the calculations assume equal charge density on both facets, $n_1 = n_2 = 1 \times 10^{11} \text{ cm}^{-2}$, neglecting spin for simplicity. By choosing the Landau gauge $\mathbf{A} = (0, Bx, 0)$, momentum k_y is a good quantum number, and the dispersion $E_m(k_y)$ results from the eigenvalue problem of Eq. 1 for $\psi_m = \phi_m(x, z)e^{ik_y y}$, where m is the Landau index.

Fig. 1(c) shows the dispersion plotted versus projected orbit centre $x_c = k_y l_B^2$ for the lowest energy levels ($l_B = \sqrt{\hbar/eB}$ is the magnetic length.) For comparison, the dispersion of a right-facing sharp QH edge [17] is shown in blue for a hard wall positioned at the vertical dotted-blue line, mirrored by the red dispersion of a left-facing edge. These two hard-wall-like dispersions arise because the sudden 90° bend in the heterojunction barrier serves as a hard wall for the incident electrons within the opposing facet. Unlike the planar antiwire of Ref. [12], there is no physical barrier separating the two systems, and the QH edges from the two orthogonal facets interpenetrate. The third subsystem is a deeply bound wire seen previously in Hartree calculations as a 1D accumulation of charge at the corner[15] and indicated here by the green parabolic dispersion. Because the corner curvature in the experimental sample [$R < 10 \text{ nm}$ from Fig. 1(b)] is significantly less than the Fermi wavelength ($\lambda_F = 70 \text{ nm}$), these Hartree calculation are expected to correctly approximate the sample potential. This accumulation wire adds two spin-degenerate 1D modes to the edge in each direction and serves as an additional 1D channel for scattering. Together with the 1D edge modes from the quantum Hall systems we therefore anticipate as many as $N = \nu + 2$ 1D modes in each direction: QH edges are by definition 1D [5, 6], and the accumulation wire consists of 1D magnetoelectric subbands [18].

We now experimentally investigate the bent QH system. Zero-resistance minima in the longitudinal resistance R_{xx} for both facets in Fig. 2 (grey) identify the gapped filling fractions where QH edge states arise: $\nu = 1/3, 2/3, 1, 2, 3, 4, 5, 6$. The conductance

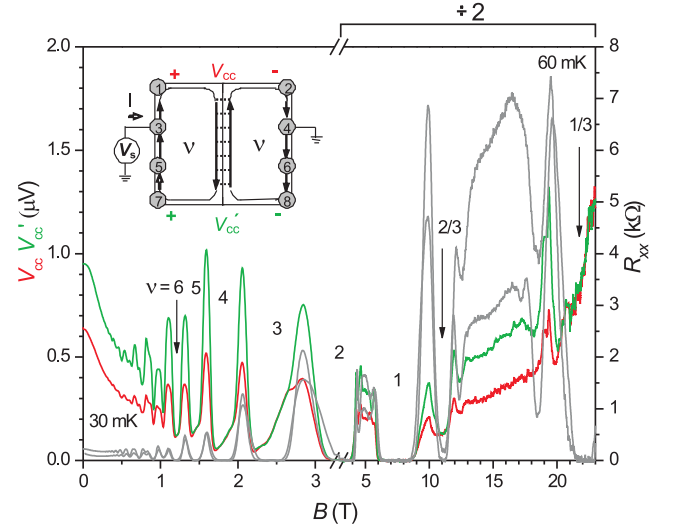


FIG. 2: (Sample A) Longitudinal resistance R_{xx} ($R_{1-7,3-5}, R_{2-8,4-6}$) within each facet (grey), and cross-corner voltages V_{cc} (red) and V'_{cc} (green). Non-zero V_{cc} minima indicate finite conduction along the junction. Inset: schematic of counter-propagating directions of current flow (arrows) contributing to 1D conduction in the presence of backscattering and interactions (dotted lines). The current I is supplied at V_s on the left facet and grounded on the opposite facet, inducing cross-corner voltages V_{cc} (red) and V'_{cc} (green).

along the corner is measured using the following 4-point geometry[13, 14]: a current I is driven across the corner to ground with an applied bias V_s , and the resultant voltage is measured between two contacts, one on each facet (Fig. 2, inset).

The cross-corner voltage $V_{cc} = V_1 - V_2$ is plotted in red in Fig. 2 ($V'_{cc} = V_7 - V_8$ in green). With the facets in a gapped QH state, the net current along the corner can be calculated to be [19] $I_{\text{wire}} = (\nu e^2/h)V_{cc} = (\nu e^2/h)V'_{cc}$. Note that $V_{cc} = V'_{cc}$ whenever $R_{xx} = 0$ thus representing that the current entering the junction is equal to the current exiting. The conductance G along the junction is then

$$G = \frac{I_{\text{wire}}}{V_s} = \nu \frac{e^2}{h} \frac{V_{cc}}{V_s} = \nu \frac{e^2}{h} \frac{V'_{cc}}{V_s} \quad (2)$$

The junction conductance for Sample A is calculated from Eq. 2 and plotted versus ν in Fig. 3(a) for filling factors where $R_{xx} = 0$. At 30 mK, the wire does not conduct for either $\nu = 1$ or 2. At $\nu = 3, 4, 5$, and 6 the wire conductance falls within the range 0.01- 0.04 of e^2/h . The fractional QH effect $\nu = 2/3$ shows a similar conductance, while the conductance at $\nu = 1/3$ at 60 mK is slightly higher. In all cases, the small junction conductance $G \ll e^2/h$ indicates that charge is strongly backscattered.

In Fig. 3(a) integer ν are notated with both the Landau index m as well as spin index σ . In diffusive 1D

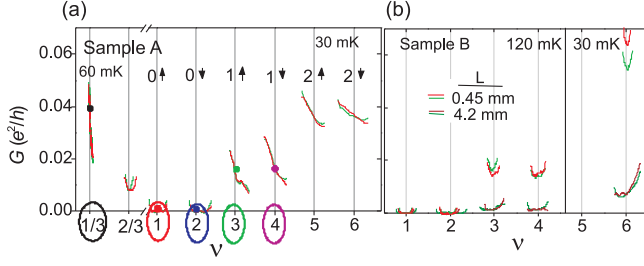


FIG. 3: Bent QH junction conductance G vs. filling factor ν from Eq. 2. (a) (Sample A) Landau index m and spin quantum number σ are noted above each integer ν revealing a pairwise similarity. Circled ν are measured as a function of temperature and voltage in Fig. 4(a) and (b). (b) (Sample B) Length dependence of the bent QH junction conductance G . The $L_1 = 4.2$ mm corner-junction was first characterized (dark red and green), and then scribed to a length $L_2 = 0.45$ mm and remeasured (light red and green).

systems, one would expect a stepwise increase in conductance with each additional mode, but instead a pair-wise behaviour in Fig. 3 seems to depend only on the Landau index m : $\nu = 1, 2$ ($m = 0$); $3, 4$ ($m = 1$); and $5, 6$ ($m = 2$). The conductance behaves as though the number of modes at the junction is not tied to the facet filling factor, but rather the facet Landau index. This would be the case if spin splitting were suppressed at this sharp QH junction. A similar lack of spin-splitting at the at a sharp edge was already experimentally observed in tunneling experiments of sharp-edge systems [17] and deserves further scrutiny.

The length dependence L of the conductance for Sample B is shown in Fig. 3(b). At $\nu = 3, 4$, and 6 , where the dependence could be measured, the short junction ($L_2 = 0.45$ mm) conducts better than the long junction ($L_1 = 4.2$ mm), with conductance scaling approximately as $G \sim 1/L$. If backscattering is distributed uniformly along the length of the junction, 1D conductance can be written $G = (e^2/h)l_0N/L$ where l_0N is the mean free path times the number of modes. These results suggests mean-free path $l_0N = 7\mu\text{m}$ ($\nu = 3, 4$) and $l_0N = 27\mu\text{m}$ ($\nu = 6$) at the temperatures shown, and indicate that the charge backscattering is distributed along the junction.

The junction conductance was also measured as a function of temperature and dc voltage bias. Fig. 4(a) shows the temperature dependence of the corner conductance for $\nu = 1/3, 1, 2, 3$, and 4 . For each ν , the same behaviour occurs across the entire minimum. With decreasing temperature T , the conductivity of the corner wire either decreases ($\nu = 1, 2$), stays roughly constant ($\nu = 3, 4$), or increases ($\nu = 1/3$), illustrating what we label as strongly insulating, weakly insulating or metallic 1D behaviour, respectively. In Fig. 4(b), the differential conductance dI/dV of the corner QH junction is plotted for the same ν as a function of dc voltage bias V_s . The insulator dI/dV drops drastically with reduced bias ($\nu = 1$,

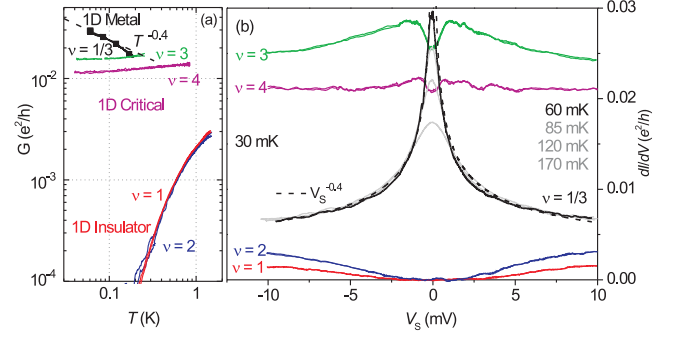


FIG. 4: Sample A: (a) The temperature dependence of the bent QH junction conductance G vs. T at the ν circled in Fig. 3. $\nu = 1, 2$ are strongly insulating; $\nu = 3, 4$ weakly insulating; and the fractional $\nu = 1/3$ metallic. (b) The dc voltage dependence V_s of the differential conductance dI/dV for the same ν . For $\nu = 1/3$ four temperatures are shown, whose peak values at $V_s = 0$ correspond to the black squares in panel (a). Power laws $T^{-0.4}$ and $V_s^{-0.4}$ plotted for comparison (dotted line).

2), whereas the metallic state dI/dV increases, forming a cusp at zero bias ($\nu = 1/3$). Varying the temperature up to 170 mK while measuring this cusp shows that most of the temperature dependence occurs at the small biases. The weakly insulating phase ($\nu = 3, 4$) shows the weakest bias dependence, with a mild dip at low bias indicating an insulator.

The three experimentally observed phases can be discussed in terms of the calculated 1D dispersions as in Fig. 1(c). An explanation for the insulator at $\nu = 1, 2$ is twofold. It can arise either from an anticrossing band insulator at the corner or from localization of 1D states. Gaps in the dispersion arise whenever the bands of Fig. 1(c) anticross, and if the Fermi level sits within such a gap, the junction would host a 1D band insulator. At higher B relevant for $\nu = 1, 2$, the anticrossing gaps from Eq. 1 are observed to increase, and are more likely to result in a 1D band insulator. Alternately, the $\nu = 1, 2$ insulator could arise according to the scaling theory of localization for 1D systems, since all 1D systems are expected to become insulators in the presence of disorder [20] and repulsive interactions [21, 22]. The limited temperature range of the data in Fig. 4(a,b) is insufficient to identify which of these two mechanisms may be responsible for the insulator observed here, though we note that the conductance does drop faster than a power-law, consistent with both explanations. We also note that the $\nu = 1, 2$ temperature dependences perfectly overlap, suggesting a common mechanism.

An explanation for the weakly insulating behaviour at $\nu = 3, 4$ is likely to fall within a weak localization picture. Examining the voltage dependence in Fig. 4(b), the zero-bias dip in dI/dV suggest a crossover from a metal to a weakly insulating state below $V_s \sim 1$ mV. This 1 meV may represent the energy scale for a 1D weak local-

ization crossover. A careful modelling of the multimode wire conductance of Fig. 1(c) will be the first step in identifying the relevant energy scales in the problem, which promises to be an interesting subject of future work.

Perhaps most surprising is the metallic behaviour at $\nu = 1/3$, with a rising junction conductance at lower temperatures. At $\nu = 1/3$ the conduction along the junction should remain 1D, comprised now of 1D fractional edges and 1D wire magnetosubbands. Looking at the temperature dependence of the voltage bias curves in Fig. 4, it is clear that the scattering is strongly temperature dependent at extremely low temperatures. The likeliest low-energy candidate for such scattering is electron-electron interactions. As discussed in Refs. [13] and [14], coupled fractional QH channels can result in exactly this sort of metallic 1D behaviour, as long as electrons (not fractional quasiparticles) backscatter the charge between the counterpropagating chiral $\nu = 1/3$ edges, creating a so-called antiwire. The T -dependence is metallic since low-temperature correlations at $\nu = 1/3$ suppress electron tunnelling and therefore suppress backscattering. The wire conductance is predicted [14] to behave as a power-law $G(T) \sim T^\alpha$, and the data of Fig. 4 would fit an exponent $\alpha = -0.4$, corresponding to the Luttinger parameter $g = 1 - \alpha/2 = 1.2$ after Ref. [14]. We note that the same exponent occurs in the voltage dependence $dI/dV \sim V^\alpha$ [dashed line, Figs. 4(a) and (b)]. If this explanation is applicable, it would appear that the 1D accumulation wire effectively functions as a "vacuum" for the counterpropagating fractional quasiparticles, permitting only electrons to backscatter. We remark that the planar antiwire geometry originally suggested in Refs. [13], [14] and implemented in Ref. [12] actually prohibits the desired strong coupling of fractional QH edges, since the intervening barrier exponentially suppresses tunnelling at high B [23]. Only in the non-planar geometry introduced here can counterpropagating edge modes overlap sufficiently in real space that the large backscattering limit may occur.

In conclusion, we have demonstrated evidence of a new type of QH system, the bent QH junction. Hartree calculations indicate that the conducting states in the junction at the Fermi energy should be 1D, and show how non-planar 1D coupling differs from planar. The temperature and voltage dependence of the junction conductivity change with ν , revealing metallic, weakly insulating, and strongly insulating states. The length dependence reveals the influence of disorder. The possible observation of a metallic 1D "antiwire" highlights the importance of interactions. This bent QH junction may help map out generic properties of 1D conductors since the metallic or insulating character is selected with an external parameter, the magnetic field.

This work was supported by DFG Quanten-Hall-Schwerpunkt-Programm and EEC funding Contract No.

RITA-CT-2003-505474. M.G. is grateful to the von Humboldt Foundation for additional support, and also thanks T. Giamarchi, W. Kang, Eun-Ah Kim, A. MacDonald, D. Polyakov, and I. Safi for illuminating conversations, Joel Moser for the SEM picture, and Martin Geisler for measurement expertise.

* Present address: Universität Regensburg, Institut für Experimentelle und Angewandte Physik, 93040 Regensburg, Germany.

- [1] A. Yacoby, H. L. Stormer, K. W. Baldwin, L. N. Pfeiffer and K. W. West, *Solid State Comm.* **101**, 77 (1997).
- [2] D. Kaufman, Y. Berk, B. Dwir, A. Rudra, A. Palevski and E. Kapon, *Phys. Rev. B* **59**, R10433 (1999).
- [3] S. B. Field, M. A. Kastner, U. Meirav, J. H. F. Scott-Thomas, D. A. Antoniadis, H. I. Smith and S. J. Wind, *Phys. Rev. B* **42**, 3523 (1990).
- [4] S. Tarucha, T. Honda and T. Sako, *Solid State Comm.* **94**, 413 (1995).
- [5] B. I. Halperin, *Phys. Rev. B* **25**, 2185 (1982).
- [6] X.-G. Wen, *Phys. Rev. Lett.* **64**, 2206 (1990).
- [7] S. Roddaro, V. Pelligrini, F. Beltram, G. Biasiol, L. Sorba, R. Raimondi and G. Vignale, *Phys. Rev. Lett.* **90**, 046805 (2003); S. Roddaro, V. Pelligrini, F. Beltram, G. Biasiol and L. Sorba, *Phys. Rev. Lett.* **93**, 046801 (2004).
- [8] Y. Ji, Y. Chung, D. Sprinzak, M. Heiblum, D. Mahalu and H. Shtrikman, *Nature* **422**, 415 (2003).
- [9] R. J. Haug, A. H. MacDonald, P. Streda and K. v. Klitzing, *Phys. Rev. Lett.* **61**, 2797 (1988).
- [10] D. B. Chklovskii, B. I. Shklovskii and L. I. Glazman, *Phys. Rev. B* **46**, 4026 (1992).
- [11] C. de C. Chamon and X.-G. Wen, *Phys. Rev. B* **49**, 8227 (1994).
- [12] W. Kang, H. L. Stormer, L. N. Pfeiffer, K. W. Baldwin and K. W. West, *Nature* **403**, 59 (2000).
- [13] S. R. Renn and D. P. Arovas, *Phys. Rev. B* **51**, 16832 (1995).
- [14] C. L. Kane and M. P. A. Fisher, *Phys. Rev. B* **56**, 15231 (1997).
- [15] M. Grayson, D. Schuh, M. Huber, M. Bichler and G. Abstreiter, *Appl. Phys. Lett.* **86**, 032101 (2005).
- [16] Growth protocol for Sample A is 05-23-02.4L3a, and sample B is 01-30-03.2L3a.
- [17] M. Huber, M. Grayson, M. Rother, W. Biberacher, W. Wegscheider and G. Abstreiter *Phys. Rev. Lett.* **94**, 016805 (2005).
- [18] B. J. van Wees, L. P. Kouwenhoven, H. van Houten, C. W. J. Beenaker, J. E. Mooij, C. T. Foxon and J. Harris, *Phys. Rev. B* **38**, 3625 (1988).
- [19] M. Buttiker, *Phys. Rev. B* **38**, 9375 (1988).
- [20] E. Abrahams, P. W. Anderson, D. C. Licciardello and T. V. Ramakrishnan, *Phys. Rev. Lett.* **42**, 673 (1979).
- [21] T. Giamarchi and H. J. Schulz, *Phys. Rev. B* **37**, 325 (1988).
- [22] I. V. Gornyi, A. D. Mirlin and D. G. Polyakov, *Phys. Rev. Lett.* **95**, 206603 (2005).
- [23] M. Grayson, D. C. Tsui, L. N. Pfeiffer, K. W. West and A. M. Chang, *Phys. Rev. Lett.* **86**, 2645 (2001).